ELSEVIER

Materials Science and Engineering 294–296 (2000) 211–216

MATERIALS SCIENCE & ENGINEERING A

www.elsevier.com/locate/msea

Z-contrast imaging of decagonal quasicrystals: an atomistic model of growth

Yanfa Yan [a,*], S.J. Pennycook [b,1]

[a] *National Renewable Energy Laboratory, 1617 Cole Boulevard, Golden, CO 80401, USA*
[b] *Oak Ridge National Laboratory, Solid State Division, PO Box 2008, Oak Ridge, TN 37831-6030, USA*

Received 20 September 1999; accepted 13 January 2000

Abstract

The structure of Al–Ni–Co decagonal quasicrystals is studied by atomic-resolution *Z*-contrast imaging technique. We propose that the presence of "rotational ordering" is the key reason leading to the formation of the 2 nm clusters and the overlaps necessary in the coverage model. Every detail of the *Z*-contrast images of the 2 nm clusters can be reproduced by a *superposition* of *rotational variants* of the 2 nm clusters seen in the ordered τ^2-inflated $Al_{13}Co_4$ approximant phase. Introducing this rotational ordering, it is clear how one cluster can nucleate neighboring clusters. Continuing this process automatically generates all the intercluster separations necessary for quasiperiodic tiling. © 2000 Elsevier Science B.V. All rights reserved.

Keywords: *Z*-contrast imaging; Decagonal quasicrystal; $Al_{72}Ni_{20}Co_8$; Rotational ordering

1. Introduction

Decagonal quasicrystals can be described by a single columnar cluster with overlaps [1–7]. The advantage of this description is that it gives some physical insight into how the quasicrystalline state may actually grow, which has been a key question since the discovery of quasicrystals [8]. The single columnar cluster in Al-based decagonal quasicrystals is the so-called 2 nm cluster. Thus, the understanding of how the 2 nm clusters form is the first step for understanding how and why these quasicrystals form. Many structure models have been proposed for the 2 nm clusters in Al-based decagonal quasicrystals based on experimental determinations and theoretical predictions [1–4,9–13]. So far, however, there is no generally accepted explanation of the origin of the 2 nm clusters, or for the particular overlaps observed, or even of the differences from crystalline approximant phases.

In this paper we investigate the structure of basic, high-perfection, Ni-rich decagonal $Al_{72}Ni_{20}Co_8$ quasicrystals [14] using the *Z*-contrast imaging technique. The *Z*-contrast images show several features distinct from the related approximant phase, specifically, closely spaced pairs of atomic columns on both the Al and transition metal sublattices, and chemical ordering in the central ring of some 2 nm clusters. We show that every detail of these clusters is reproduced by a *superposition* of *rotational variants* of the 2 nm clusters seen in the τ^2-inflated $Al_{13}Co_4$ approximant. Introducing this rotational ordering, it is clear how one cluster can nucleate neighboring clusters. Continuing this process *automatically* generates all the intercluster separations necessary for quasiperiodic tiling.

2. *Z*-contrast imaging

The principle of *Z*-contrast imaging in the scanning transmission electron microscope (STEM) is shown schematically in Fig. 1 [15–17]. A small electron probe is scanned across a thin specimen, and the *Z*-contrast image results from mapping the intensity of electrons reaching the annular detector. The probe size in our VG Microscopes HB603U is 1.3 Å full-width-half-maximum intensity, enabling us to image individual atomic columns down to that separation. The high scattering angles not only break the coherence in the transverse plane, but also through the thickness of the crystal, giving a monotonically increasing image intensity with

* Corresponding author. Tel.: +1-303-384-6456; fax: +1-303-384-6604.
E-mail address: yyan@nrel.gov (Y. Yan).
[1] Co-corresponding author.

0921-5093/00/$ – see front matter © 2000 Elsevier Science B.V. All rights reserved.
PII: S0921-5093(00)01309-5

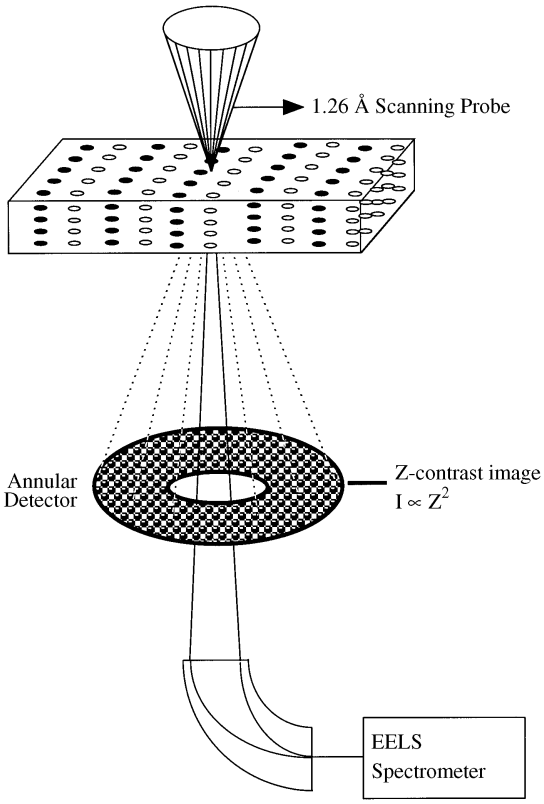

Fig. 1. Schematic showing a fine probe formed by the objective lens of an STEM. As the probe scans the specimen, the high angle scattering is mapped out to give the *Z*-contrast image.

thickness. The resulting images are therefore relatively intuitive to interpret: atomic columns contribute to the image with a brightness determined primarily by their mean square atomic number *Z*. This chemical sensitivity enables us to distinguish different elements directly at the atomic scale. Unlike the coherent imaging of conventional high-resolution electron microscopy, the positions of atomic columns can be determined directly and uniquely from the image to a high accuracy, without the need for extensive image simulations of model structures or image reconstruction procedures. Incoherent imaging effectively bypasses the phase problem of high-resolution electron microscopy (HREM), a particular advantage for complex materials. Thus, in an image of an Al-TM (TM: transition metal) decagonal quasicrystal, TM columns will show as the brightest features and Al columns will show as less bright features. In both cases the local intensity maximum is closely correlated with the column position.

3. Results and discussion

It has long been recognized that detailed knowledge of atom positions is a prerequisite to understanding the quasicrystalline structure and its formation mechanism, in particular the relationship between quasicrystals and their crystalline approximant phases. A number of recent studies have provided significant insights into the differences and relationships between the structures of the quasicrystalline and approximant phases. A common feature of the Al-based decagonal quasicrystals (e.g. Al–Ni–Fe, Al–Ni–Co, Al–Cu–Co, etc.) is that they consist of distinct 2 nm clusters. Fig. 2 shows a *Z*-contrast image of the high-perfection decagonal $Al_{72}Ni_{20}Co_8$ quasicrystal, taken along the periodic axis. The distinct 2 nm clusters are clearly seen as indicated by black circles. Because of the smaller probe size of our instrument, we are able to see more details of the structure than previous *Z*-contrast studies [9,10]. Most importantly, both the TM (here Co and Ni) *and the Al* (aluminium) columns are resolved, and can be distinguished by their strong *Z*-contrast. The very bright spots correspond to the columns of the TM while weaker intensity maxima or saddle points correspond to Al atoms. It is seen that the 2 nm ring has 10 closely spaced pairs of columns (one pair is indicated by two arrows). This is the most important feature that was not observed in previous work.

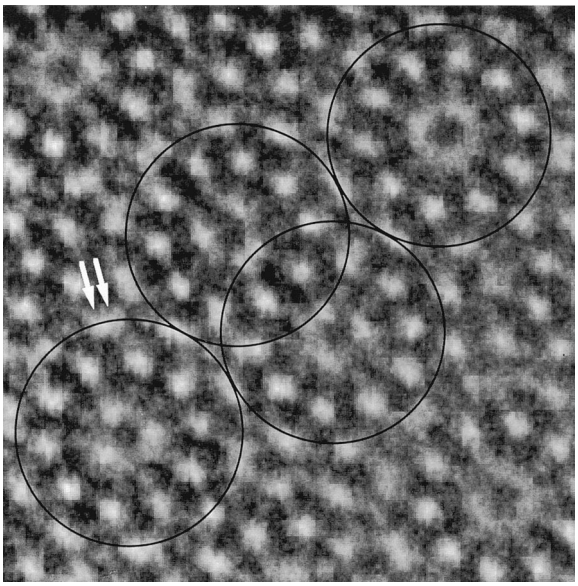

Fig. 2. *Z*-contrast image of $Al_{72}Ni_{20}Co_8$ viewed along the tenfold axis. The black circles indicate the 2 nm clusters.

It has been reported that a 2 nm cluster also exists in the τ^2-inflated $Al_{13}Co_4$ approximant phase [18]. The 2 nm cluster is composed of five pentagonal atomic clusters, each of which consists of five TM columns, shown as large circles in Fig. 3(a). This pentagonal atomic cluster exists in all other approximants [19]. The τ^2-inflated $Al_{13}Co_4$ approximant phase has a periodicity of 0.8 nm along the columnar axis. Thus, the structure of the 2 nm clusters has four layers (see Fig. 6 of Ref. [18]). However, it is seen that in the layer at

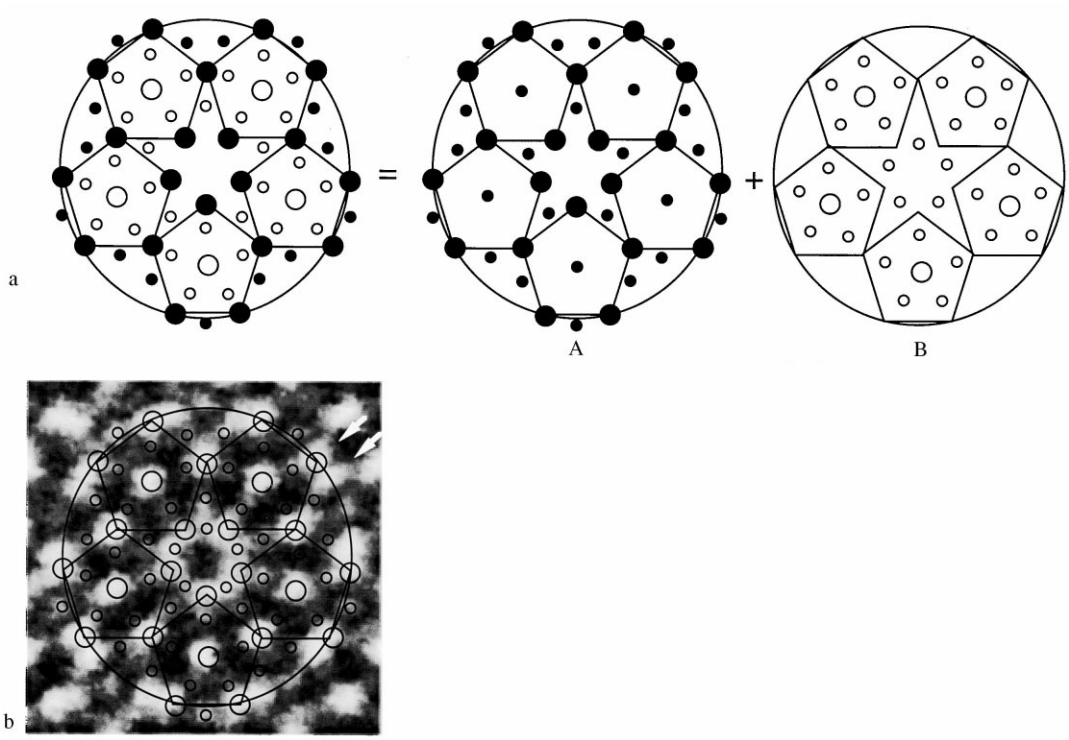

Fig. 3. (a) The structure of the new 2 nm clusters obtained from those in the τ^2-inflated $Al_{13}Co_4$ crystalline approximant. Large circles denote transition metal columns, small circles Al columns. (b) Superimposition shows how the structure of the new 2 nm cluster fits *precisely half* the columns in the central and outer rings of the quasicrystal.

$z = \frac{1}{2}$, the Al columns have no symmetry. If the ordering was the same in the layer at $z = 0$ and the layer at $z = \frac{1}{2}$, the approximant phase would have only two different layers with a periodicity of 0.4 nm. Fig. 3(a) shows the structure of a phase consisting only of the A and B layers of the approximant (the same as the layers at $z = 1$ and $\frac{1}{4}$ of Fig. 6 in Ref. [18]). The positions of the Al columns are similar to those in $Al_{13}Fe_4$, whose structure is known to consist of a stacking of ordered and disordered pentagonal clusters [20,21]. In Fig. 3(b), we superimpose this structure onto the image of the quasicrystal. All the TM and Al columns in the structure are present in the image, which justifies our assumed Al positions in the basic cluster. However, two rings in the quasicrystal are seen to have a significantly different structure, containing many features not present in the new cluster.

All the missing sites can be explained by simply rotating the cluster through 36° to form a *rotational variant*, as shown in Fig. 4(a). The structure is identical to that proposed previously [22], but now explains the origin of the 10 columns in the central ring and the 10 closely spaced TM column pairs around the 2 nm ring. It also explains the 10 closely spaced pairs of Al columns in the third ring from the center which are not visible by eye, but whose presence was previously detected by line traces and confirmed by image simulations [22]. The new 2 nm cluster in Fig. 4(a) has four layers stacked as ABA′B′, where A′ and B′ denote the 36° rotation of layers A and B, respectively. Thus, the simple operation shown in Fig. 4(a) would give a periodicity of 0.8 nm along the periodic axis. But it is known that $Al_{72}Ni_{20}Co_8$ is a high-perfection decagonal quasicrystal, with no diffuse scattering in electron diffraction and a periodicity of 0.4 nm [14]. Thus, the rotational ordering operation in $Al_{72}Ni_{20}Co_8$ is not as simple as that shown in Fig. 4(a). Fig. 4(b) is another possible rotational ordering operation, which gives a stacking sequence of AA′BB′. Though the projection of this stacking sequence fits the *Z*-contrast image, it still gives a 0.8 nm periodicity. Thus, we propose that the rotational ordering in $Al_{72}Ni_{20}Co_8$ occurs *within the individual layers* as shown in Fig. 4(c). Each layer (A and B) is split into two half-occupied layers, and one is rotated by 36° with respect to the other. After introducing this rotational ordering operation in each layer, two kinds of new layers A″ and B″ are formed as shown in Fig. 4(c). Now, since every site has half occupancy, not only does the projected structure fit the *Z*-contrast image, it also gives a 0.4 nm periodicity. We emphasize that the closely spaced pairs of Al and TM columns seen experimentally *must* be partially occupied (i.e. phason flip sites) since their separation of ~0.13 nm is too small to allow both sites to be occupied in the same atomic layer. The quasicrystalline structure may thus represent a true superposi-

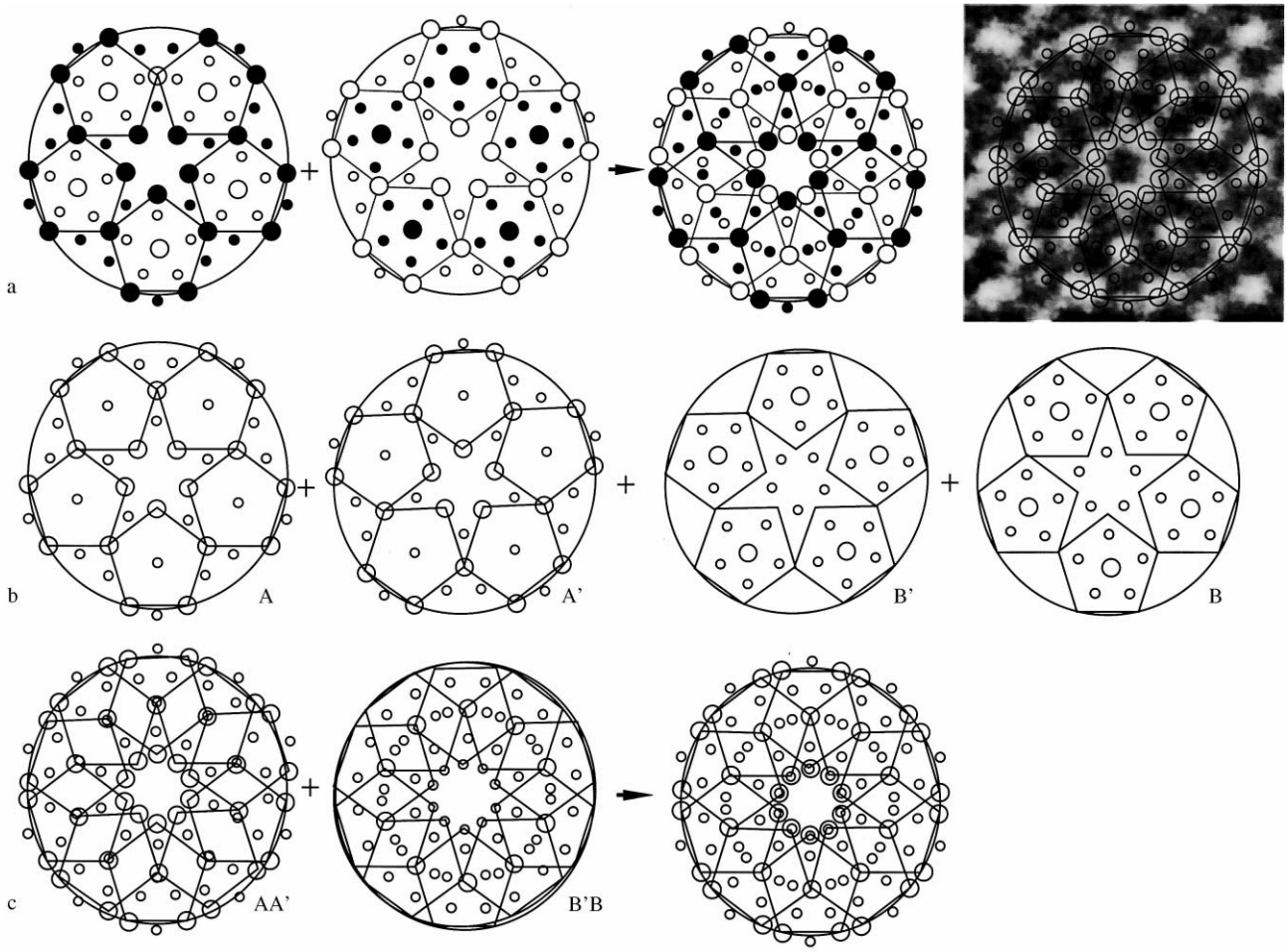

Fig. 4. (a) Two rotational variants of the basic 2 nm cluster obtained from the τ^2-inflated $Al_{13}Co_4$ approximant are superimposed. The resulting cluster superimposed on the *Z*-contrast image gives a perfect fit. However, these two rotational variants give a new periodicity of 0.8 nm. (b) A different rotational ordering operation which also gives a 0.8 nm periodicity. (c) Rotational ordering is introduced into each individual layer. This results in a 0.4 nm periodicity, consistent with electron diffraction results.

tion of the two rotational variants of the basic 2 nm cluster derived from the approximant phase. Such a structure would naturally contain a high chemical entropy explaining the high temperature stability of this basic Ni-rich decagonal phase.

The most important feature of our new cluster is that it naturally provides an atomistic explanation of how a quasiperiodic phase can grow. The central rings of the clusters contain pairs of closely spaced TM columns similar to the pairs present in the outer ring. This naturally suggests how one cluster can nucleate a second, as shown in Fig. 5(a). For the overlap shown, most of the sites for the second cluster already exist in the first.

If we now repeat the same growth process, the third cluster can take several specific orientations with respect to the first, as shown in Fig. 5(b)–(d). In particular, our growth model naturally results in several different overlaps with intercluster separations in the ratio τ, 0.74, 1.23, 2.06 and 3.44 nm. The first two are precisely as required in the Gummelt coverage model of the ideal quasicrystal, and the remaining two result automatically.

Thus our growth model naturally accounts for all the overlaps required to define the ideal quasiperiodic state, as well as every detail in our *Z*-contrast images. Although we developed this growth model in the context of the near-perfect decagonal phase, our clusters have great freedom to form overlaps, and our growth model may well apply to random tiling also. It differs fundamentally from the quasi-unit-cell model which predicts a unique tiling structure. In the case of the approximant phase, if we try to overlap its fully ordered clusters it is difficult to find a high density of common sites. This suggests that the approximant phase grows by the addition of *individual* small pentagonal units around the basic 2 nm cluster, as found by Saitoh et al. [18] in the case of the τ^2-inflated $Al_{13}Co_4$ approximant. Thus, we believe that the existence of rotational ordering is fundamental to stabilizing the quasicrystalline form.

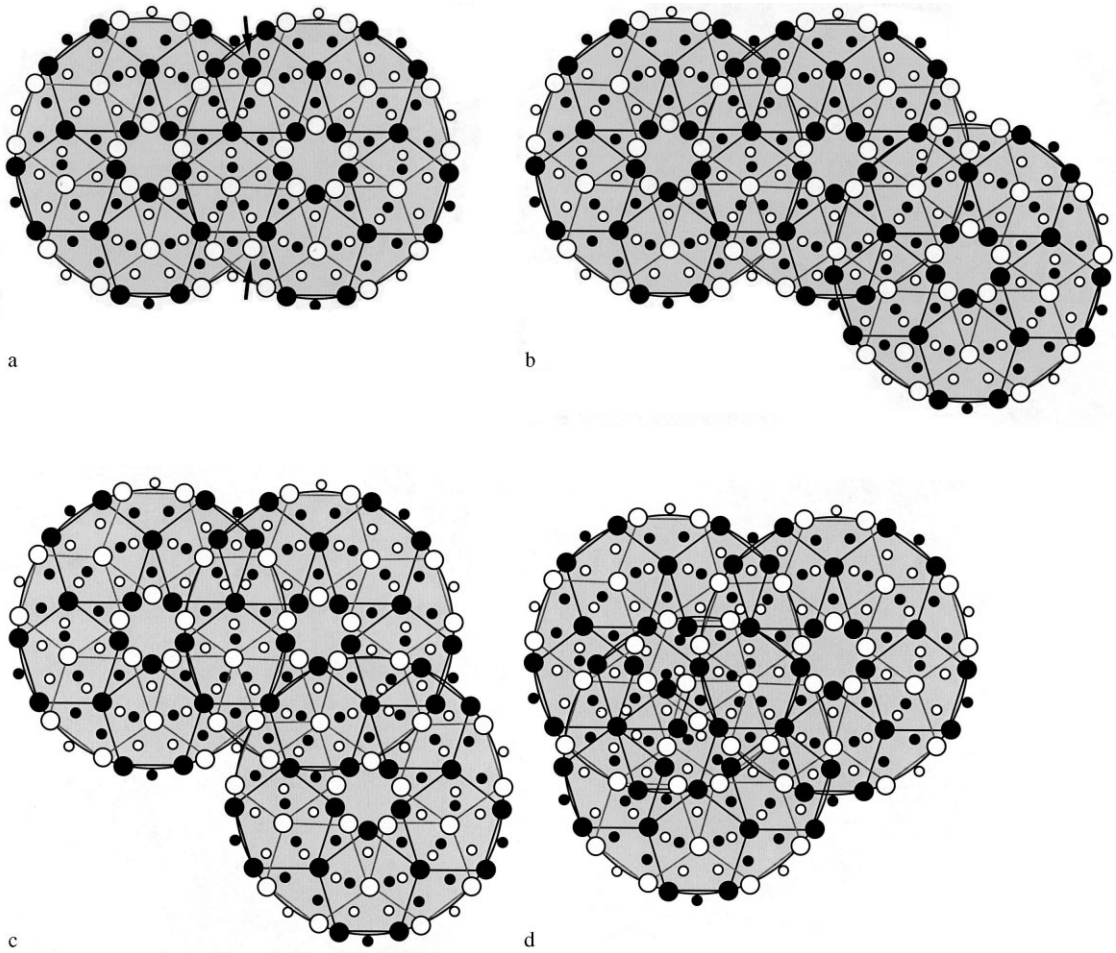

Fig. 5. (a) Our complex cluster structure provides a natural explanation for nucleation of a second cluster overlapping the first, resulting in a 1.23 nm intercluster spacing. Most of the sites in the overlap region are common to both — the only exceptions are columns in the closely spaced pairs shown arrowed. (b)–(d): Continuing this nucleation mechanism leads to intercluster spacings of (b) 3.44 nm, (c) 2.06 nm, and (d) 0.74 nm.

4. Conclusions

We have presented a growth mechanism for decagonal quasicrystals: The quasicrystalline structure forms as a consequence of growth under conditions that lead to *rotational ordering*. Introducing this rotational ordering, it is clear how one cluster can nucleate neighboring clusters. Most significantly, continuing this process automatically generates all the intercluster separations necessary for the coverage model, thus providing an atomistic insight into the underlying cause of the quasiperiodic state.

Acknowledgements

This work was supported by the US Department of Energy under contract No. DE-AC36-83CH10093 at NREL, and DE-AC05-96OR22464 at ORNL. We thank Prof. W. Steurer for stimulating discussions, Dr. A.P. Tsai of the National Research Institute for Metals, Japan for the provision of high-perfection decagonal $Al_{72}Ni_{20}Co_8$ quasicrystal studied in this paper, and J.N. Pennycook for helpful overlaps.

References

[1] W. Steurer, Acta Crystallogr. B 45 (1989) 534.
[2] W. Steurer, K.H. Kuo, Acta Crystallogr. B 46 (1990) 703.
[3] S.E. Burkov, Phys. Rev. Lett. 67 (1991) 614.
[4] K. Hiraga, F.J. Lincoln, W. Sun, Mater. Trans. Jpn. Inst. Met. 32 (1991) 308.
[5] M. Duneau, in: Proceedings of the Fifth International Conference on Quasicrystals, World Scientific, Singapore, 1995, p. 116.
[6] P. Gummelt, Geometriae Dedicata 62 (1996) 1.
[7] P.J. Steinhardt, H.-C. Jeong, Nature 382 (1996) 433.
[8] D. Shechtman, I. Blech, D. Gratias, J.W. Cahn, Phys. Rev. Lett. 53 (1984) 1951.
[9] K. Saitoh, K. Tsuda, M. Tanaka, K. Kaneko, A.-P. Tsai, Jpn. J. Appl. Phys. 36 (1998) L1404.
[10] P.J. Steinhardt, H.-C. Jeong, K. Saitoh, M. Tanaka, E. Abe, A.-P. Tsai, Nature 396 (1998) 55.
[11] K. Saitoh, K. Tsuda, M. Tanaka, A.-P. Tsai, A. Inoue, T. Masumoto, Philos. Mag. A 73 (1996) 387.
[12] E. Cockayne, M. Widom, Phys. Rev. Lett. 81 (1998) 598.

[13] A. Yamamoto, Sci. Rep. Res. Inst., Tohoku Univ. A 42 (1996) 207.
[14] S. Ritsch, C. Beeli, H.-U. Nissen, T. Gödecke, M. Scheffer, R. Lück, Philos. Mag. Lett. 74 (1996) 99.
[15] S.J. Pennycook, D.E. Jesson, Phys. Rev. Lett. 64 (1990) 938.
[16] S.J. Pennycook, P.D. Nellist, in: D. Rickerby, G. Valdré, U. Valdré (Eds.), Impact of Electron Scanning Probe Microscopy on Materials Research, Kluwer Academic Publishers, The Netherlands, 1999, VCH Publishers, Weinheim, 1997, 595 pp.
[17] D.E. Jesson, S.J. Pennycook, Proc. Roy. Soc. A 449 (1995) 273.
[18] K. Saitoh, T. Yokosawa, M. Tanaka, A.-P. Tsai, J. Electron Microsc. 48 (1999) 105.
[19] Z.M. Mo, H.X. Sui, X.L. Ma, K.H. Kuo, Metall. Mater. Trans. A 29 (1998) 1565.
[20] P.J. Black, Acta Crystallogr. 8 (1955) 43.
[21] P.J. Black, Acta Crystallogr. 8 (1955) 175.
[22] Y. Yan, S.J. Pennycook, A.-P. Tsai, Phys. Rev. Lett. 81 (1998) 5145.